journal

J. Am. Ceram. Soc., 88 [4] 903–906 (2005)
DOI: 10.1111/j.1551-2916.2005.00163.x

Yield Strength of α-Silicon Nitride at High Pressure and High Temperature

J. Qian,† C. Pantea, J. Zhang, L. L. Daemen, and Y. Zhao

Lansce-12, MS H805, Los Alamos National Laboratory, Los Alamos, New Mexico 87545

M. Tang

MST-8, MS G755, Los Alamos National Laboratory, Los Alamos, New Mexico 87545

T. Uchida and Y. Wang

Center for Advanced Radiation Sources, The University of Chicago, Illinois 60637

Through the analysis of peak broadening of energy-dispersive diffraction lines from a powdered sample, the yield strength of α-Si_3N_4 was investigated at a pressure of 9 GPa and temperatures up to 1234°C. During compression at room temperature, the lattice strain deduced from peak broadening increased linearly with pressure up to 9.2 GPa, with no clear indication of strain saturation. While heating at 9 GPa, diffraction peaks narrowed and significant stress relaxation was observed at temperatures above 400°C, indicating the onset of yielding. The yield strength of α-Si_3N_4 decreases rapidly with increasing temperature: from 8.7 GPa at 400°C to 4.0 GPa at 1234°C. The low temperature for the onset of yielding and decrease of yield strength upon further heating bring up concern regarding the performance of α-Si_3N_4 as an engineering material. Finally, the grain size variation is also outlined together with the dependence of differential strain on pressure and on temperature. This provides crucial information for clarifying the "fine structure" of the evolution of the differential strain.

I. Introduction

Because of its covalent bonding, silicon nitride (Si_3N_4) exhibits high hardness, high wear resistance, low electrical conductivity, extraordinary chemical inertness, and high thermal stability.[1–3] Today, Si_3N_4 is one of the key engineering ceramics widely used in machining and in the semiconductor and aerospace industries. In addition to the development of fabrication techniques such as hot pressing,[4,5] gas pressure sintering,[6] high pressure/high temperature sintering,[7] and chemical vapor deposition methods,[8] sustained efforts have been devoted to discovering new phases of Si_3N_4 experimentally[9–12] and to elucidating the fundamental electronic structure and bonding theoretically.[13,14] Four polymorphs of Si_3N_4 have been reported so far, including two hexagonal phases (α- and β-Si_3N_4), a cubic spinel structure (c-Si_3N_4), and another still-ambiguous phase (δ-Si_3N_4).[10] Extensive work has been performed in studying the mechanical properties,[15–18] phase transition,[19–21] and equation of state[22] of Si_3N_4. However, one of the fundamental parameters of Si_3N_4—the yield strength at high pressure/high temperature conditions—is still lacking. This information is critical for evaluating the performance of Si_3N_4 in a real working (load and high-temperature) environment. In this work, we investigate the yield strength of α-Si_3N_4 at pressures up to 9.2 GPa and temperatures up to 1234°C through the analysis of the shape of X-ray diffraction lines from a powdered sample.

II. Experimental Procedure

α-Si_3N_4 powder (purity >90%, grain size 50–100 nm) was purchased from Alfa Aesar (Ward Hill, MA). Two separated layers of α-Si_3N_4 and NaCl powder were loaded inside a hexagonal BN capsule, which was placed in an amorphous carbon furnace. NaCl worked as the internal pressure standard and pressure was calculated from Decker's equation of state for NaCl.[23] The temperature was measured by a $W_{25}Re_{75}$–W_3Re_{97} thermocouple that was positioned at the center of the furnace and was in direct contact with the α-Si_3N_4 sample and NaCl layers; no correction was made for the pressure effect on the thermocouple emf. *In situ* energy-dispersive synchrotron X-ray diffraction experiments were performed at the bending magnet beamline (13-BM-D) at the GSECARS facility of the Advanced Photon Source using the 250-ton multi-anvil press with the DIA-type cubic anvil apparatus.[24] The incident X-ray beam was collimated to a rectangular cross-section with dimensions 100 μm × 200 μm, and the diffracted X-ray signal was collected by a Ge solid-state detector at a fixed angle of $2\theta = 5.857°$. The sample was compressed to 9.2 GPa at room temperature and then heated to 1234°C under constant load. The X-ray diffraction patterns were collected at α-Si_3N_4 and NaCl locations very close to the thermocouple junction at different pressure–temperature conditions. The obtained energy-dispersive diffraction data were analyzed with the Plot85 software package.

The stress and strength of α-Si_3N_4 can be derived from the peak broadening in the X-ray diffraction patterns. The detailed method is outlined by Weidner *et al.*[25] based on two facts: microscopic deviatoric stress is the origin of X-ray line broadening in addition to grain size, and yielding occurs through the redistribution of the deviatoric stress over the entire sample at a certain high stress level. In the case of diffraction lines with Gaussian profiles, the combination of grain size and strain broadening can be described by:[26]

$$[\beta(E)]^2 = \left[\frac{Khc}{2L\sin\theta}\right]^2 + (\varepsilon E)^2$$

where $\beta(E)$ is the peak broadening at the photon energy E, K the Scherrer constant, h Planck's constant, c the velocity of light, L

I. Tanaka—contributing editor

Manuscript No. 10882. Received February 26, 2004; approved August 29, 2004.
The Los Alamos National Laboratory research projects supported by the DoE-OIT_IMF and DoD/DoE_MOU programs.
Work at Argonne National Laboratory supported by the National Science Foundation—Earth Sciences (EAR-0217473), Department of Energy—Geosciences (DE-FG02-94ER14466), and the State of Illinois.
Use of the APS is supported by the U.S. Department of Energy, Basic Energy Sciences, and Office of Energy Research, under Contract No. W-31-109-Eng-38.
†Author to whom correspondence should be addressed. e-mail: jiangq@lanl.gov

the average grain size, and ε the differential strain. Therefore, differential strain and average grain size can be derived from the slope and ordinate intercept of the plot of $[\beta(E)]^2$ against E^2, respectively.

III. Results and Discussion

The (110) and (101) diffraction peaks of α-Si_3N_4 are displayed in Fig. 1 at four different points along the experimental pressure–temperature path. During the compression from ambient up to 9.2 GPa at room temperature, the α-Si_3N_4 peaks broaden asymmetrically, with a much more severe broadening on the small d-spacing side of the peak—see the bottom three curves in Fig. 1. This indicates that the applied pressure is supported only by the bridged parts of the α-Si_3N_4 grains. Meanwhile, at this stage, the generated stress is not large enough to cause any yielding. Similar behavior was observed for diamond and moissanite during compression up to 10 and 11.8 GPa, respectively.[25,27] During heating at constant load, both (110) and (101) peaks of α-Si_3N_4 remained almost unchanged up to 400°C. The peaks narrow and become more symmetric at temperatures above 400°C, which is a clear evidence of yielding accompanied by stress redistribution over the entire sample—see the top two curves in Fig. 1.

Figure 2 shows the plot of $[\beta(E)]^2$ as a function of E^2 for two selected pressure–temperature conditions. Because of the co-existence of the NaCl pressure standard, h-BN capsule, and α-Si_3N_4 in the sample chamber, diffraction peaks from these different phases tend to overlap, and this complicates the extraction of peak width, especially with broadened peaks at high-pressure conditions. For better statistics, five α-Si_3N_4 diffraction lines are selected for peak broadening analysis, and the error bar represents the standard deviation. There are relatively large

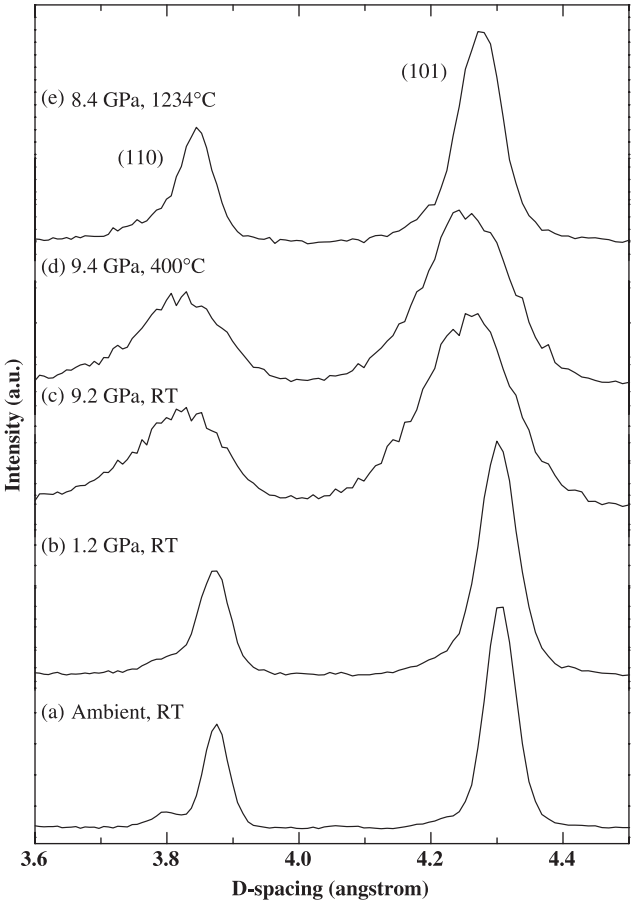

Fig. 1. (110) and (101) diffraction lines of α-Si_3N_4 at selected pressure and temperature conditions: (a) ambient, room temperature, (b) 1.2 GPa, room temperature, (c) 9.2 GPa, room temperature, (d) 9.4 GPa, 400°C, and (e) 8.4 GPa, 1234°C.

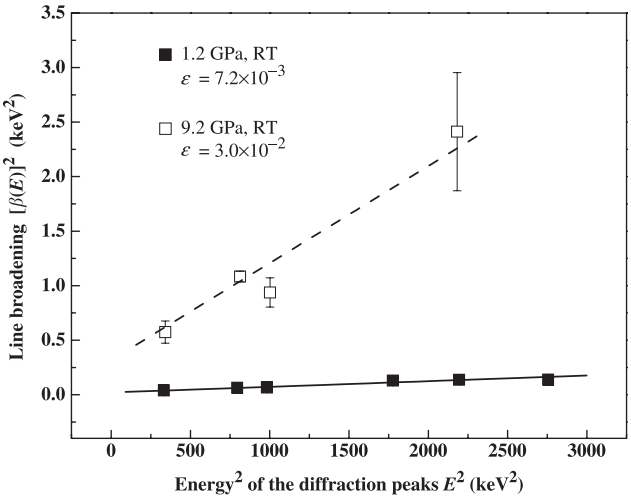

Fig. 2. Energy-dependent line broadening of α-Si_3N_4 at two different pressures at room temperature: full square fitted with solid line—1.2 GPa and blank square fitted with dash line—9.2 GPa.

uncertainties about the line broadening of some of the α-Si_3N_4 peaks, but it is still obvious that a linear fit is suitable for the plot of $[\beta(E)]^2$ against E^2 even for the worst-case scenario, shown as the top blank square plot fitted with a dashed line in Fig. 2. Better precision of line broadening and more accurate deduction of grains size and differential strain can be obtained with angle-dispersive diffraction and monochromatic synchrotron beam, which requires a much more complicated instrumentation for the multi-anvil press.

The grain size, especially when it goes down to nanometer range, contributes significantly to the diffraction line broadening.[28] Given the intrinsic brittleness of the α-Si_3N_4,[2,5,17] we believe it was worthwhile to explore possible grain size reduction during compression. Additionally, we thought that more details about the dependence of the differential strain as a function of pressure and/or temperature could be revealed by introducing the grain size in the same plot.

Figure 3 shows the differential strain and average grain size at various pressure and temperature conditions as full- and blank-square plots with solid and dashed guide lines, respectively. The nearly linear dependence of the strain on pressure up to 9.2 GPa at room temperature indicates that the compression process is elastic. The plateau around the pressure of 3 GPa is clearly associated with a dramatic grain size reduction approximately from 80 to 30 nm. It is intuitive to envision that grain fracture

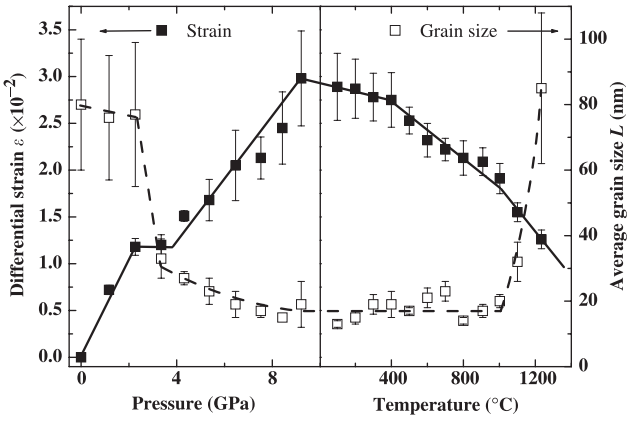

Fig. 3. Differential strain (full square) and average grain size (blank square) of α-Si_3N_4 at various pressure and temperature conditions: left plot—compression at room temperature; right plot—heating at constant load corresponding to a pressure of 9 GPa. The differential strain and average grain size are derived from the slope and *Y*-ordinate intercept of the linear fitting, respectively, shown in Fig. 2. The lines are meant to guide the eye only.

rearranges local grain-to-grain contact and eases the strain growth temporarily at this particular region during loading. Afterward, there is an average grain size reduction from 30 to 20 nm upon further compressing from 3.4 to 9.2 GPa, but it seems that this small grain size reduction has no effect on the dependence of differential strain on pressure.

As temperature is increased to 400°C at constant load, there is a slight negative slope in the differential strain, which is probably caused by thermally induced strain relaxation because there is a small increase in the internal cell pressure in this region. Above 400°C, α-Si_3N_4 starts yielding and the strain drops rapidly with further heating to 1234°C. It is essential to point out here that α→β-Si_3N_4 transformation is an important issue at high pressure/high temperature conditions,[19–21] and there is no apparent α→β-Si_3N_4 transformation in our experiment up to 8.4 GPa and 1234°C. The grain size of α-Si_3N_4 remains around 20 nm upon heating all the way to 1000°C, above which there is a fast grain growth. The final grain size at 1234°C is about 80 nm, which is very close to the initial grain size. Rapid grain growth (by about one order of magnitude) has been reported around 1000°C during the crystallization of amorphous Si_3N_4.[7] Simultaneously, at 1000°C, the strain starts decreasing more rapidly. This coincidence can be explained by α-Si_3N_4 grain growth (which should be facilitated by the presence of small grains at that stage of the experiment). Indeed, grain growth reduces grain-to-grain contact sites and accelerates the differential strain diminution. For α-Si_3N_4, the preceding results clearly demonstrate that the grain size information is critical in understanding the detailed evolution of differential strain at high pressure/high temperature. It is necessary to mention that the average grain size here is the X-ray scattering domain size (crystallite size), which may not represent the crystal size of α-Si_3N_4. Further experimental investigations in other ceramics are needed to confirm the importance of simultaneously determining stress and grain size in differential strain studies.

Given that the differential stress that can be sustained by the grains represents the yield strength after the yielding of α-Si_3N_4 at 400°C, the yield strength of α-Si_3N_4 can be determined by multiplying the differential strain by its aggregate Young's modulus, 315 GPa, which is calculated from the bulk modulus of 229 GPa based on the equation of state study by Kruger *et al.*[22] and a Poisson's ratio of 0.27.

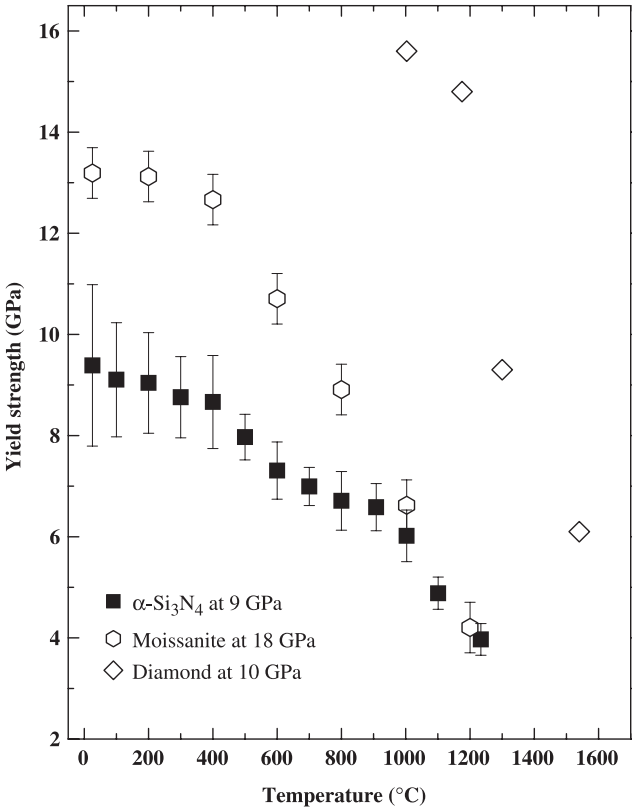

Fig. 4. Yield strength of α-Si_3N_4 (square) as a function of temperature at a pressure of 9 GPa. The strength data for moissanite (hexagon) and diamond (diamond) are also plotted for comparison.

The yield strength of α-Si_3N_4 as a function of temperature at 9 GPa is shown in Fig. 4. Data for moissanite and diamond are also plotted for comparison. The yield strength of α-Si_3N_4 decreases from 8.7 GPa at 400°C to 4.0 GPa at 1234°C. Compared with the yield strength of moissanite (12.8 at 400°C),[27] α-Si_3N_4 is much weaker at relatively low temperatures (below 800°C). The comparison with diamond (with yield strength above 16 GPa at the onset temperature of 1000°C) is even less favorable.[25] A comparison of the hardness and Young's modulus of α-Si_3N_4 and moissanite makes the observed differences between the materials at least plausible. The Vickers hardness of α-Si_3N_4 is only half that of moissanite, and the Young's modulus is approximately 70% of that of moissanite. On the other hand, the yield strength of α-Si_3N_4 is about the same as that of moissanite at temperatures above 1000°C, which can be attributed to a strong resistance to thermally induced weakening. It should be pointed out that the pressures during heating at constant load are quite different, 18 GPa in the study of moissanite and 9 GPa in this work.

IV. Conclusions

We demonstrated the dependence of strain on pressure and temperature through the analysis of peak broadening of the energy-dispersive diffraction data for α-Si_3N_4. The "fine structure" of the evolution of strain can be explicated with the complementary information delivered by the grain size variation. The yield strength of α-Si_3N_4 is low initially (less than 9 GPa at 400°C). Although it becomes comparable with moissanite at temperatures above 1000°C, the low onset temperature of yielding (400°C) and the deterioration of strength upon further increase of temperature will set a limitation on the performance of α-Si_3N_4 as an engineering material. Nevertheless, a better understanding of the correlation between yield strength and grain size could be extremely helpful in the near future in designing functional ceramics through a deliberate configuration of grains with various sizes.

Acknowledgments

This work was completed under the auspices of the U.S. Department of Energy (DoE) under contract W-7405-ENG-36 with the University of California. The experimental part of this work was performed at GeoSoilEnviroCARS (Sector 13), Advanced Photon Source (APS), Argonne National Laboratory.

References

[1]A. Kelly and N. H. Macmillan, *Strong Solids*. Oxford University Press, New York, 1986.
[2]J. B. Wachtman, *Mechanical Properties of Ceramics, Chapter 24*. John Wiley & Sons, New York, 1996.
[3]A. J. Pyzik and D. F. Carroll, "Technology of Self-Reinforced Silicon Nitride," *Annu. Rev. Mater. Sci.*, **24**, 189–214 (1994).
[4]G. Himsolt, H. Knoch, H. Huebner, and F. Kleinlein, "Mechanical Properties of Hot-Pressed Silicon Nitride with Different Grain Structures," *J. Am. Ceram. Soc.*, **62** [1–2] 29–32 (1979).
[5]I. Tanaka, G. Pezzotti, T. Okamoto, and Y. Miyamoto, "Hot Isostatic Press Sintering and Properties of Silicon Nitride Without Additives," *J. Am. Ceram. Soc.*, **72**, 1656–60 (1989).
[6]M. Mitomo and S. Uenosono, "Gas Pressure Sintering of β-Silicon Nitride," *J. Mater. Sci.*, **26**, 3940–4 (1991).
[7]Y. Li, Y. Liang, F. Zheng, X. Ma, and S. Cui, "Sintering of Nanopowders of Amorphous Silicon Nitride Under Ultrahigh Pressure," *J. Mater. Res.*, **15** [4] 988–94 (2000).
[8]J. Yota, J. Hander, and A. A. Saleh, "A Comparative Study on Inductively-Coupled Plasma High-Density Plasma, Plasma-Enhanced, and Low Pressure Chemical Vapor Deposition Silicon Nitride Films," *J. Vac. Sci. Technol. A*, **18** [2] 372–6 (2000).
[9]A. Zerr, G. Miehe, G. Serhgiou, M. Schwarz, E. Kroke, R. Riedel, H. Fueb, P. Kroll, and R. Boehler, "Synthesis of Cubic Silicon Nitride," *Nature*, **400**, 340–2 (1999).

[10]A. Zerr, "A New High-Pressure δ-Phase of Si_3N_4," *Phys. Stat. Sol. (b)*, **227** [2] R4–6 (2001).
[11]T. Sekine, H. He, T. Kobayashi, M. Zhang, and F. Xu, "Shock-Induced Transformation of β-Si_3N_4 to a High-Pressure Cubic-Spinel Phase," *Appl. Phys. Lett*., **76** [25] 3706–8 (2000).
[12]M. Schwarz, G. Miehe, A. Zerr, E. Krobe, B. T. Poe, H. Fuess, and R. Riedel, "Spinel-Si_3N_4: Multi-Anvil Press Synthesis and Structural Refinement," *Adv. Mater*., **12** [12] 883–7 (2000).
[13]S. Mo, L. Ouyang, W. Y. Ching, I. Tanaka, Y. Koyama, and R. Riedel, "Interesting Physical Properties of the New Spinel Phases of Si_3N_4 and C_3N_4," *Phys. Rev. Lett*., **83** [24] 5046–9 (1999).
[14]W. Y. Ching, L. Ouyang, and J. D. Gale, "Full ab initio Geometry Optimization of All Known Crystalline Phase of Si_3N_4," *Phys. Rev. B*., **61** [13] 8696–700 (2000).
[15]I. Tanaka, F. Oba, T. Sekine, E. Ito, A. Kubo, K. Tatsumi, H. Adachi, and T. Yamamoto, "Hardness of Cubic Silicon Nitride," *J. Mater. Res*., **17** [4] 731–3 (2002).
[16]J. Z. Jiang, H. Lindelov, L. Gerward, K. Stahl, J. M. Recio, P. Mori-Sanchez, S. Carlson, M. Mezouar, E. Dooryhee, A. Fitch, and D. J. Frost, "Compressibility and Thermal Expansion of Cubic Silicon Nitride," *Phys. Rev. B*., **65**, 161202(R) (2002).
[17]K. Ogawa, F. Sugiyama, G. Pezzotti, and T. Nishida, "Impact Strength of Continuous-Carbon-Fiber-Reinforced Silicon Nitride Measured by Using the Split Hopkinson Pressure Bar," *J. Am. Ceram. Soc*., **81** [1] 166–72 (1998).
[18]N. Hirosaki, Y. Akimune, and M. Mitomo, "Microstructure Characterization of Gas-Pressure Sintered β-Silicon Nitride Containing Large β-Silicon Nitride Seeds," *J. Am. Ceram. Soc*., **77** [4] 1093–7 (1994).
[19]N. V. Danilenko, G. S. Oleinik, V. D. Dobrovol'skii, V. F. Britun, and N. P. Semenenko, "Microstructural Features of the α→β Transformation in Silicon Nitride at High Pressures and Temperatures," *Sov. Powder Metall. Met. Ceram*., **31** [12] 1035–40 (1992).
[20]H. He, T. Sekine, T. Kobayashi, and H. Hirosaki, "Shock-Induced Phase Transition of β-Si_3N_4 to c-Si_3N_4," *Phys. Rev. B*., **62** [17] 11412–7 (2000).
[21]H. Suematsu, M. Mitomo, T. E. Mitchell, J. Petrovic, O. Fukunaga, and N. Ohashi, "The α–β Transformation in Silicon Nitride Single Crystals," *J. Am. Ceram. Soc*., **80** [3] 615–20 (1997).
[22]M. B. Kruger, J. H. Nguyen, Y. M. Li, W. A. Caldwell, M. H. Manghnani, and R. Jeanloz, "Equation of State of α-Si_3N_4," *Phys. Rev. B*., **55** [6] 3456–60 (1997).
[23]D. L. Decker, "High-Pressure Equation of State for NaCl, KCl and CsCl," *J. Appl. Phys*., **42**, 3239–44 (1971).
[24]D. J. Weidner, M. T. Vaughan, J. Ko, Y. Wang, X. Liu, A. Yeganeh-haeri, R. E. Pacalo, and Y. Zhao, "Characterization of Stress, Pressure and Temperature in SAM85, a DIA Type High Pressure Apparatus;" pp. 13–17 in *High-Pressure Research: Application to Earth and Planetary Sciences*, **Vol. 67**, Edited by Y. Syono and M. H. Manghnani. Geophysics Monograph Series, AGU, Washington, DC, 1992.
[25]D. J. Weidner, Y. Wang, and M. T. Vaughan, "Strength of Diamond," *Science*, **266**, 419–22 (1994).
[26]L. Gerward, S. Morup, and H. Topsoe, "Particle Size and Strain Broadening in Energy-Dispersive X-ray Powder Patterns," *J. Appl. Phys*., **47** [3] 822–5 (1976).
[27]J. Zhang, L. Wang, D. J. Weidner, T. Uchida, and J. Xu, "The Strength of Moissanite," *Am. Mineral*., **87**, 1005–8 (2002).
[28]H. P. Klug and L. E. Alexander, *X-Ray Diffraction Procedures for Polycrystalline and Amorphous Materials*. John Wiley & Sons, New York, 1974. □